

Modelling the effect of white matter microstructure on gradient echo signal evolution

Benjamin Tendler¹, Samuel Wharton¹, and Richard Bowtell¹

¹Sir Peter Mansfield Imaging Centre, University of Nottingham, Nottingham, Nottinghamshire, United Kingdom

Introduction: The evolution of the magnitude and phase of gradient echo (GE) signals is sensitive to white matter (WM) microstructure^{1,2}. This effect has been characterised by using a three-pool model of WM, comprised of axonal, myelin and external compartments, which can be most simply described by using a triple-exponential decay with different compartmental resonant frequency offsets³. The signal can be more accurately described by using geometric fibre models in which the spatially varying resonant frequency offsets are calculated from analytic expressions¹ (Fig. 1). Here we compare the magnitude and phase signals produced using these different models and show that the triple-exponential model can be improved in the static dephasing regime by adding in terms which approximately account for frequency variation in the myelin and external compartments. We also demonstrate the effects of including a range of fibre sizes and diffusion in a multiple-fibre model.

Theory: The signal from the simple, three-pool model can be represented as³:

$$S = A_a e^{i\langle\omega_a\rangle TE - \frac{TE}{T_{2a}^*}} + A_m \rho e^{i\langle\omega_m\rangle TE - \frac{TE}{T_{2m}^*}} + A_e e^{-\frac{TE}{T_{2e}^*}} \quad (1)$$

(parameter definitions in Box 1, $\langle\omega\rangle$ values derived using Ref.¹). This model can provide a reasonable approximation of the GE signal from WM, but does not properly account for the effect of frequency variation in the myelin and external pools evident in Fig. 1. To approximate this effect, compartmental signals can be weighted by additional terms, $e^{-\frac{1}{2}D_m TE^2}$ (myelin) and $e^{-\frac{1}{2}D_e TE^2}$ (external). Here, D_m and D_e are related to the variance of the field in each compartment:

$$D_m = \left(\chi_A^2 \left[\frac{9}{16} - \frac{9}{16} (\Lambda + \Lambda^2) (\ln(G))^2 + \frac{1+g^2}{128} + \frac{1}{32} \Lambda \ln(G) \right] + \frac{\chi_I \chi_A}{8} \left(\Lambda \ln(G) + \frac{g^2}{16} \right) + \chi_I^2 \left(\frac{g^2}{8} \right)^2 \right)^2 \sin^4 \theta \gamma^2 B_0^2 \quad (2)$$

$$D_e = \frac{FVF}{8} |X_D|^2 \gamma^2 B_0^2 \sin^4 \theta \quad (3)$$

Method: The signals from six different models were compared: the original triple-exponential model (Eq. 1); triple-exponential model with myelin dephasing term (Eqs. 1&2), triple-exponential with external dephasing term (Eqs. 1&3); triple-exponential with both myelin & external terms (Eqs. 1-3); single-fibre and multi-fibre models (Fig. 1). The multi-fibre model was formed in a 2000x2000 array initially with fixed axonal radius of 12 pixels. Parameters for all the simulations were taken from previous work¹ (Box 2). The root mean squared difference (RMSD) over the 50ms evolution time between signals generated using the triple-exponential models and single-fibre model compared with the multi-fibre model were then evaluated for a range of myelin and external pool T_2^* -values ($T_{2m}^* = 4 - 20$ ms, $T_{2e}^* = 25 - 50$ ms). To examine the properties of the multi-fibre model in more detail, simulated signals were compared for models with (i) identical fibre sizes (1 μm axonal diameter) and (ii) a distribution of fibre diameters representative of the genu of the corpus callosum⁵ (with fixed g-ratio and FVF), for the cases of no diffusion and diffusion in the external and axonal compartments ($D = 10^{-9} \text{ m}^2 \text{s}^{-1}$). Diffusion was incorporated via a two-dimensional random walk with reflection at the myelin boundaries.

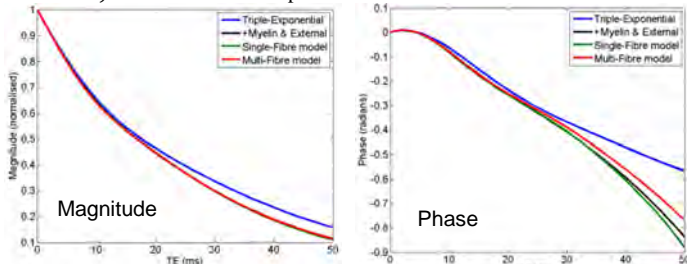


Fig. 2: Magnitude & phase evolution for 4 different models.

Results & Discussion:

Fig. 2 displays the magnitude and phase variation for the triple-exponential model (with and without additional dephasing terms) and the single & multi-fibre models, produced using the parameters in Box 2. The plots indicate that inclusion of the myelin and external dephasing terms greatly improves the agreement between the three-pool model and the full multi-fibre model at longer TE values in the static dephasing regime. There is good agreement between the single and multiple-fibre model, small differences are due to the single-fibre model not capturing the effect of frequency variation in the axonal compartment due to fields from adjacent fibres. The RMSD plots in Fig. 3 further emphasise the importance of including the dephasing terms in the three-pool model. Inclusion of D_e has the largest effect on the RMSD, indicating that dephasing in the external compartment is the main cause of discrepancy. Inclusion of the myelin dephasing effect further improves the agreement with the multi-fibre model, with D_m having an increasing effect as T_{2m}^* increases so that the myelin signal contribution persists to longer dephasing times. Fig. 4 shows the effects of diffusion on the signal phase from the multi-fibre model; these are most apparent at higher TE, partly due to the dominance of myelin water decay at low TE values. Use of a realistic distribution of fibre sizes (fixed g-ratio) has a small effect on the phase evolution at large TE, which is eliminated by diffusion. Diffusion reduces the attenuation of the signal contribution from the external pool due to phase dispersion: the three-pool model with myelin dephasing consequently also characterises the signal from a more realistic multi-fibre model with diffusion. The ambition of future work is to examine this model further to quantify the effects of varying other factors, including g-ratio and FVF, along with the development of a 3D multi-fibre model to examine effects caused by crossing fibres.

References: 1. Wharton, S. and Bowtell, R. *PNAS* **109**, 18559-18564 (2012)., 2. Sati, P. et al. *NIMG* **77**, 268-278, (2013)., 3. Van Gelderen, P. et al. *MRM* **67**, 110-117 (2012)., 4. Wharton, S. and Bowtell, R. *NIMG* **83**, 1011-1023 (2013)., 5. Aboitiz, F. et al. *Brain Research* **598**, 143-153 (1992).

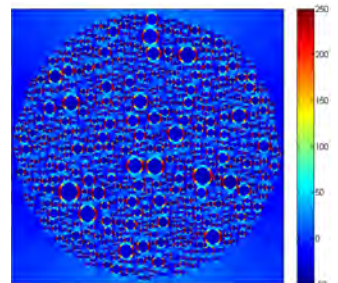


Fig. 1: Variation of α (rads) at TE for the multi-fibre model.

Box 1: Variables in triple exponential model

S = Complex signal, $A_{a,m,e}$, $T_{2a,m,e}^*$, $\langle\omega_{a,m,e}\rangle$ = relative amplitude, T_2^* & average frequency of the axonal, myelin and external pools¹, ρ = relative water content of myelin pool, FVF = fibre volume fraction; $g = g\text{-ratio}$, $G = g^{-1}$, $\Lambda = G^2/1 - G^2$, $\chi_{I/A}$ = isotropic and anisotropic susceptibility of myelin, E = exchange offset, $X_D = (\chi_I + \chi_A/4) \times (1 - G^2)$, θ = angle between fibre(s) and B_0 .

Box 2: Parameter values¹: $\rho = 0.7$, $T_{2a}^* = 36$ ms, $T_{2m}^* = 8$ ms, $T_{2e}^* = 36$ ms, $\chi_I = -100$ ppb, $\chi_A = -100$ ppb, $E = 20$ ppb, $g = 0.8$, FVF = 0.5, $\theta = 90^\circ$.

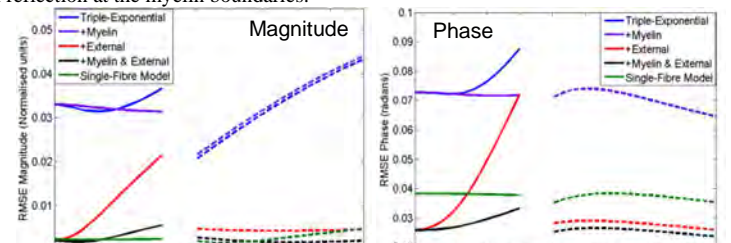


Fig. 3: RMSD values for magnitude and phase data compared to a multi-fibre model. Solid lines correspond to fixed T_{2e}^* & varying T_{2m}^* ; dashed lines fixed T_{2m}^* & varying T_{2e}^* .

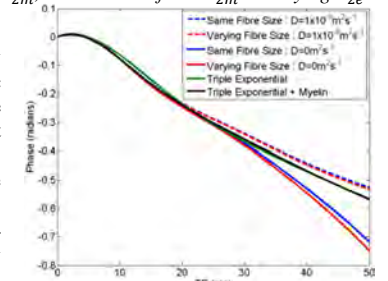


Fig. 4: Effect of diffusion on phase.